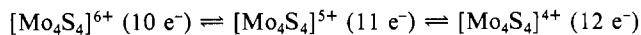


Figure 1. ORTEP drawing of $\text{Mo}_4\text{S}_4(\text{HB}(\text{pz})_3)_4(\text{pz})$ (1).

Finally, the oxidation state of the cluster deserves comment. We have previously³ isolated a 10-electron cluster from the reaction of the aquo ion with NCS^- . The title compound, on the other hand, is an 11-electron cluster. Cyclic voltammetry on the Mo_4S_4 aquo species has revealed that the interconversions²



are facile. The E^0 values in 2 M *p*-toluenesulfonic acid are +0.54 and -0.08 V (vs. NHE) for the first and second steps, respectively. This clearly indicates that all three forms are accessible in aqueous medium and interconvertible by mild oxidants or reductants. It is therefore conceivable that $\text{KHB}(\text{pz})_3$ is acting not only as a ligand but also as a reducing agent similar to NaBH_4 , which was successfully employed in the reduction of $[\text{Mo}_4\text{S}_4(\text{edta})_2]^{3-}$.

Acknowledgment. We thank the National Science Foundation for support.

Registry No. 1, 103619-49-4.

Supplementary Material Available: Tables of anisotropic displacement parameters and complete bond distances and angles (4 pages); a listing of structure factors (7 pages). Ordering information is given on any current masthead page.

Contribution from the Department of Chemistry, University of Massachusetts, Amherst, Massachusetts 01003, and Department of Molecular Spectroscopy, Research Institute of Materials, University of Nijmegen, Toernooiveld, 6525 ED Nijmegen, The Netherlands

Relation between Structure and Magnetic Exchange Pathways in Hexakis(pyridine *N*-oxide)copper Complexes

J. S. Wood[†] and C. P. Keijzers*[‡]

Received April 4, 1986

The hexakis(pyridine *N*-oxide) complexes $\text{M}(\text{PyO})_6\text{X}_2$ ($\text{M} = \text{Mn}^{2+} - \text{Zn}^{2+}$; $\text{X} = \text{ClO}_4^-, \text{BF}_4^-, \text{NO}_3^-$) crystallize in space group $R\bar{3}$, with S_6 point symmetry for the octahedral complex ions. The anions have threefold symmetry.¹ The form of the antiferromagnetic exchange in the copper complexes is governed by the nature of the cooperative Jahn-Teller effect operative in the

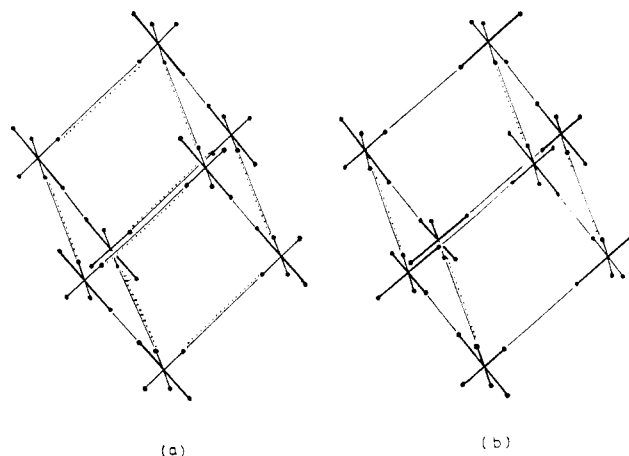


Figure 1. Rhombohedral unit cell of $\text{Cu}(\text{PyO})_6^{2+}$ octahedra showing the low-temperature structures for (a) the ferrodistorstive fluoroborate complex and (b) the antiferrodistorstive perchlorate and nitrate complexes. Dotted lines denote the directions of principal antiferromagnetic exchange.

Table I. Unit Cell Dimensions and Calculated Shortest Intermolecular O-O Distance in $\text{M}(\text{PyO})_6\text{X}_2$ Complexes

X	M = Cu			M = Zn		
	<i>a</i> , Å	α , deg	O...O, Å	<i>a</i> , Å	α , deg	O...O, Å
ClO_4^-	9.620	81.21	5.600 ^a	9.632	81.07	5.577 ^a
	9.450	80.84	5.472 ^b			
BF_4^-	9.621	81.46	5.592 ^a	9.621	81.25	5.555 ^a
NO_3^-	9.480	83.45	5.413 ^c	9.503	83.38	<i>d</i>

^aReference 1c. ^bResults from neutron diffraction at 20 K, ref 6. ^cReference 1d. ^dJ. Smits, private communication.

particular complex.² In the BF_4^- complex, the tetragonally elongated cations are ferrodistorstively ordered at low temp.^{3,4} and two-dimensional antiferromagnetism is found. In the ClO_4^- and NO_3^- complexes, the low-temperature ordering of the elongated octahedra is antiferrodistorstive^{3,4} and one-dimensional antiferromagnetic behavior is found.² The two low-temperature structures are illustrated in Figure 1. The near equivalence (circa 1 K) of the intrachain exchange in the ClO_4^- complex and the intraplane exchange in the BF_4^- complex (which are defined as the *strong* exchange, *J*, in this note) suggests that the same superexchange pathway is operative in both complexes. This path has been assumed to result from a long-range interaction (overlap?) of the oxygen atoms of the PyO ligands of neighboring complexes.² However, the pathway might also involve the pyridine rings of the ligands since the lone pair density on the oxygen atom is directed toward the rings of neighboring molecules⁵ and the oxygen-ring plane distance is only 3.28 Å at 20 K, while the O-O distance is 5.47 Å.⁶ Since these initial results, EPR measurements on pairs of complexes^{7,8} in heavily doped, diamagnetic, zinc host crystals gave important information on the small *interchain*/plane exchange (defined as *J'*) and they revealed that, for each anion, several different pair configurations are produced. The relative abundances of these pair configurations and also *J'* depend on

- (1) van Ingen Schenau, A. D.; Verschoor, G. C.; Romers, C. *Acta Crystallogr., Sect. B: Struct. Crystallogr. Cryst. Chem.* **1974**, *B30*, 1686. (b) Bergendahl, T. J.; Wood, J. S. *Inorg. Chem.* **1975**, *14*, 338. (c) O'Connor, C. J.; Sinn, E.; Carlin, R. L. *Inorg. Chem.* **1977**, *16*, 3314. (d) Wood, J. S.; Day, R. O. *Cryst. Struct. Commun.* **1981**, *10*, 255.
- (2) Algra, H.; De Jongh, L.; Carlin, R. L. *Physica B+C* **1978**, *93*, 24.
- (3) Reinen, D.; Krause, S. *Solid State Commun.* **1979**, *29*, 691.
- (4) Wood, J. S.; Keijzers, C. P.; de Boer, E.; Buttafava, A. *Inorg. Chem.* **1980**, *19*, 2213.
- (5) Wood, J. S. *Acta Crystallogr., Sect. A: Found. Crystallogr.* **1984**, *A40*, C-166. Wood, J. S. to be submitted for publication.
- (6) Keijzers, C. P.; McMullan, R. K.; Wood, J. S.; van Kalker, G.; Srinivasan, R.; de Boer, E. *Inorg. Chem.* **1982**, *21*, 4275.
- (7) Van Kalker, G.; Keijzers, C. P.; Srinivasan, R.; de Boer, E.; Wood, J. S. *Mol. Phys.* **1983**, *48*, 1.
- (8) Paulissen, M. L. H.; Keijzers, C. P. *J. Mol. Struct.* **1984**, *113*, 267.

[†]University of Massachusetts.

[‡]University of Nijmegen.

Table II. Strong Exchange Coupling Constants (J) in $\text{Cu}(\text{PyO})_6\text{X}_2$ and Weak Exchange Constants (J') and g_{\parallel} Values for $^{63}\text{Cu}/\text{Zn}(\text{PyO})_6\text{X}_2$

X	J^a	J'^a	g_{\parallel}
ClO_4^-	7089 ^b	287 ^c	2.376
BF_4^-	7645 ^b	224 ^c	2.391
NO_3^-	>7650	329 ^d	2.378

^a Units of 10^{-4} cm^{-1} . ^b Reference 2. ^c Reference 7. ^d Reference 8.

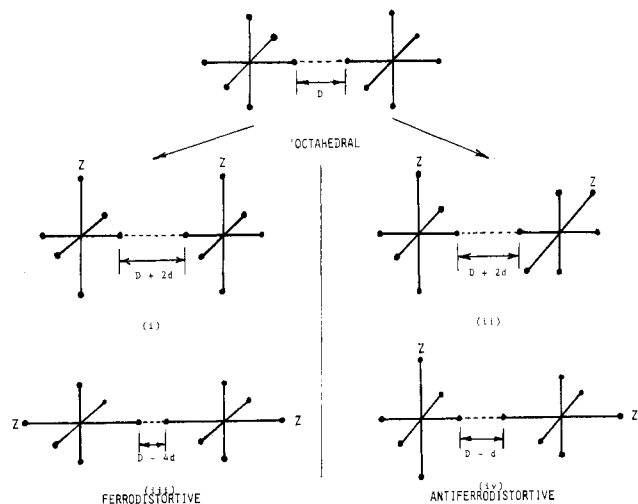


Figure 2. Variation of O...O distance in the various ferro- and antiferrodistortively ordered pairs of CuO_6 octahedra (directions of elongation denoted by z). Interactions i and ii correspond to the strongly exchange-coupled pairs (constant J) while (iii) and (iv) correspond to the weakly exchange-coupled pairs. Interaction iv has the exchange constant J' .

the anion. In addition, in the NO_3^- system antiferrodistortively ordered *next-nearest-neighbor* pairs were found, with an exchange constant roughly twice as large as the J' value of the nearest-neighbor pairs.⁸ The purpose of this paper is to point out a relationship between J and J' on one side and the magnitude of the Jahn-Teller distortion on the other from the details of the structures as revealed by X-ray and neutron diffraction. In conjunction with the structural data, observations are made regarding the role of the anion in facilitating the magnetic exchange.

Experimental Section

The majority of the EPR and structural data were reported previously.^{7,8} X-ray crystal data for $\text{Zn}(\text{PyO})_6(\text{NO}_3)_2$ were measured on an Enraf-Nonius CAD-4 diffractometer. Powder EPR spectra of the three heavily doped zinc complexes were measured at X-band frequency at 20 K on a Varian E-12 spectrometer.

Results and Discussion

Table I summarizes structural data for the pure copper and zinc complexes. Table II lists the magnitudes of J and J' and the values of g_{\parallel} as derived from the EPR powder spectra. The J' values correspond to the antiferrodistortively oriented pairs (i.e. A_1 and $C_{1,2}$ in Figure 5 of ref 7 and in Figure 3 of ref 8). Table II shows that the larger value of J is accompanied by a larger value of g_{\parallel} and a smaller J' . These results can be understood qualitatively as follows. The smaller g_{\parallel} value of the ClO_4^- complex indicates a more strongly tetragonally elongated CuO_6 moiety than in the BF_4^- complex.⁹ Now define the degree of distortion from the "averaged" octahedral Cu-O bond length to be " d " for the four contracted bonds and " $2d$ " for the two elongated bonds. Then the O...O distance for an antiferrodistortive pair with large (intra-chain) exchange, J (ii) in Figure 2), is longer by $2d$ than in the octahedrally averaged pair, and this distance is shorter by d for a pair with small (interchain) exchange, J' (iv) in Figure 2).¹⁰

(9) Keijzers, C. P.; van Kalkerem, G.; de Boer, E.; Wood, J. S. *Mol. Phys.* **1983**, *49*, 1187. The observed difference in g_{\parallel} values leads to a predicted difference $d_{\text{ClO}_4} - d_{\text{BF}_4}$ of 0.025 Å by using the results in Figure 4.

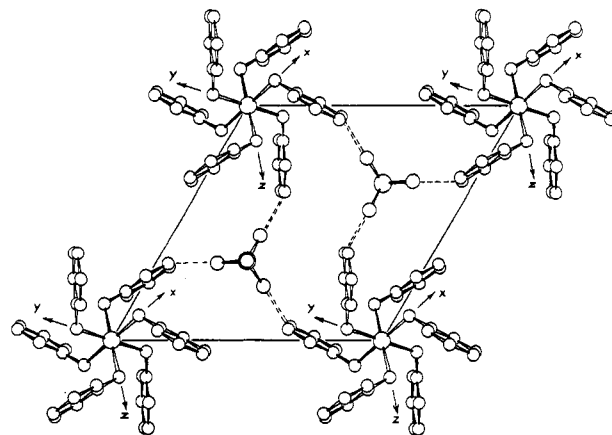


Figure 3. Projection of one layer of the structure of $\text{Cu}(\text{PyO})_6(\text{ClO}_4)_2$ onto (001) showing the hydrogen-bonding linking 3-fold-related cations. Single broken lines denote H bonds to ligands on the z axes (axis of elongation) while double broken lines denote H bonds to ligands on x and y axes.

For the ferrodistortive pairs, the O...O distance is smaller by $4d$ for the pair with J' and longer by $2d$ for the pair with J (iii) and (i) in Figure 2). (Note that configurations i, ii, and iv are of relevance for the data in Table II.) Assuming that the O...O distance is directly significant for the magnitude of J and J' , one sees that the greater the tetragonality (lower g_{\parallel} value) the larger J' and the smaller J . This is observed for the ClO_4^- and BF_4^- complexes.

For the NO_3^- complex, the O...O contact distance is expected to be smaller than for the other complexes, because of the room-temperature unit cell dimensions of the Cu and the Zn crystal and because the tetragonality (g_{\parallel}) is equal to that of the ClO_4^- system. This explains the relatively large value of J' . In addition, the J value is expected to be the largest of the three. This coupling has not been measured experimentally. However, antiferrodistortive pairs with the large exchange were observed in very low concentration in the EPR of the doped system.⁸ Since these pairs are absent in the spectra of the ClO_4^- system, this supports the conclusion. Additional support comes from the analogous cobalt complexes where also the NO_3^- system has the largest J value.¹¹

The fact that next-nearest-neighbor pairs are observed only in the NO_3^- system suggests that an additional pathway for antiferromagnetic exchange is present that is more significant in the NO_3^- system than in the other two. The exchange constant is $\sim 590 \cdot 10^{-4} \text{ cm}^{-1}$, almost the double value of the nearest-neighbor pairs! We think that the extra pathway involves the anions: the low-temperature neutron analyses of the copper⁶ and the cobalt¹² perchlorate complexes have shown the presence of rather strong C-H...O-ClO₃ bonds, involving the hydrogen atom of C(2) in the ligand ring. At 20 K the C...O and H...O distances are 3.004 (2) and 2.169 (3) Å, respectively, appreciably less than the typical values of ~ 3.25 and ~ 2.3 Å for these types of hydrogen bonds.¹³ The available room-temperature C(2)...O distance of 3.24 Å of the nitrate complex suggests the presence of hydrogen bonding in this system also. The hydrogen bonds connect threefold related $\text{Cu}(\text{PyO})_6^{2+}$ ions and so provide an exchange pathway between complexes "across" the short diagonals of the rhombohedral unit cell¹⁴ (Figure 1). Since all complex ions within one layer of the hexagonal cell have their tetragonal axes of elongation parallel (Figure 1), of the three complexes surrounding one anion,

- (10) For simplicity this analysis assumes a linear C-O...O-Cu arrangement. The actual, small, departure from linearity will not affect the argument.
 (11) Carlin, R. L.; O'Connor, C. J. *J. Am. Chem. Soc.* **1977**, *99*, 7387.
 (12) Wood, J. S.; Brown, R. K.; Lehmann, H. S. *Acta Crystallogr., Sect. C: Cryst. Struct. Commun.*, in press.
 (13) Vinogradov, S. N.; Linell, R. H. *Hydrogen Bonding*; Van Nostrand Reinhold: New York, 1971; p 177.
 (14) Magnetic exchange processes via H bond pathways have been documented previously in the literature, e.g.: Bertrand, J. A.; Black, T. D.; Eller, P. G.; Helm, F. T.; Mahmood, R. *Inorg. Chem.* **1976**, *15*, 2965.

one pair will then be "connected" through their ligands coordinated in the xy planes, i.e. the planes containing the unpaired electrons. Figure 3 illustrates that every anion "connects" a ligand on the x axis of one $\text{Cu}(\text{PyO})_6^{2+}$ complex with a ligand on the y axis from a neighboring complex. The fact that these pair spectra only occur in the NO_3^- system and not in the other two can be understood with this model since the NO_3^- ion with its π -system is well-known to provide a better exchange pathway than the tetrahedral ClO_4^- and BF_4^- ions with their sp^3 orbitals. In addition, the larger value of the coupling constant of this next-nearest-neighbor pair, relative to the nearest-neighbor interaction described by J' , can be rationalized: as described above, the former constant describes the coupling between two orbitals that contain an unpaired electron ($d_{x^2-y^2}$), while the latter describes the coupling between $d_{x^2-y^2}$ and the doubly filled d_{z^2} orbital. As a consequence, the exchange coupling is much larger although the distance between the copper centers is much larger.

Registry No. $\text{Cu}(\text{PyO})_6^{2+}$, 47839-68-9.

Contribution from the Departments of Chemistry,
University of Tennessee,
Knoxville, Tennessee 37996-1600,
and North Carolina State University,
Raleigh, North Carolina 27695-8204

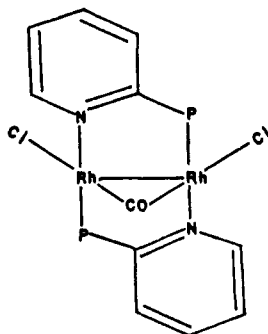
Electrosynthesis and X-ray Structure of a Dinuclear Rhodium Complex Containing a Bridging Nitrate Ion

Louis J. Tortorelli,^{1a} Craig A. Tucker,^{1b} Clifton Woods,^{*1a}
and John Bordner^{1c}

Received October 29, 1985

In recent years there has been considerable interest in dinuclear rhodium complexes containing bidentate bridging ligands where the donor atoms are those of group 15 elements.² One aspect of these complexes that has been a point of focus has been the wide range of metal-metal separations that can be achieved with ligands such as bis(diphenylphosphino)methane (dppm), bis(diphenylarsino)methane (dam), (diphenylarsino)(diphenylphosphino)methane (dapm), and 2-(diphenylphosphino)pyridine (Ph_2Ppy).

The dinuclear rhodium(I) complex $\text{Rh}_2(\mu\text{-Ph}_2\text{Ppy})_2(\mu\text{-CO})\text{Cl}_2$ (**1**) has been prepared and structurally characterized.³ It has



been noted that the geometric constraints of two bridging Ph_2Ppy ligands in a dinuclear complex limit the metal-metal separations to the metal-metal bond range,⁴ and indeed **1** contains a Rh-Rh

bond of 2.612 Å. If the bridging CO is viewed as a neutral ligand, the rhodium atoms in **1** are formally rhodium(I). When rhodium(I) dimers that lack a formal Rh-Rh bond and contain bridging dppm, dam, and dapm ligands undergo oxidative addition of molecules such as iodine, bromine, or CH_3SSCH_3 ,^{5,6} the Rh-Rh separation decreases with the formation of a Rh-Rh bond.

Due to the small number of dinuclear rhodium(II) complexes that exists with bridging dppm, dam, dapm, and Ph_2Ppy ligands, we have been interested in investigating the possibility of making rhodium(II) complexes via electrochemical oxidation and assessing the role these electron-transfer processes play in the formation and stability of the Rh-Rh bond. One comparison of potential interest is that of the rhodium-rhodium bond distances in dinuclear rhodium(I) compounds, such as **1**, and those of their dinuclear rhodium(II) derivatives. Such comparisons might shed more light on how various geometric and steric constraints and electronic factors affect the metal-metal bond distances in these dinuclear rhodium complexes.

Experimental Section

Preparation of Compounds. Procedures outlined in the literature were used to prepare Ph_2Ppy ⁷ and $\text{Rh}_2(\mu\text{-Ph}_2\text{Ppy})_2(\mu\text{-CO})\text{Cl}_2$.⁴

$\text{Rh}_2(\text{Ph}_2\text{Ppy})_2(\mu\text{-NO}_3)(\text{CO})\text{Cl}_2 \cdot \text{CH}_2\text{Cl}_2$ (2**).** Approximately 100-150 mg of $\text{Rh}_2(\mu\text{-Ph}_2\text{Ppy})_2(\mu\text{-CO})\text{Cl}_2$ was dissolved in 50 mL of CH_2Cl_2 containing 0.10 M tetra-*n*-butylammonium nitrate (TBAN) and a 5-fold molar excess of tetra-*n*-butylammonium chloride (TBAC). The solution was oxidized at 1.00 V (vs. SCE). After the oxidation was complete, the solution was washed with copious amounts of water to remove the TBAN and TBAC. The CH_2Cl_2 layer was reduced in volume on a rotary evaporator, and a greenish product was precipitated with ether and recrystallized from CH_2Cl_2 /ether (yield 70%). If the oxidized solution is stripped to dryness and the residue is dissolved in acetone, the desired product can be obtained in comparable yield by the addition of water.

This compound can also be prepared by carrying out the same procedure as outlined above excluding the TBAC. Under these conditions, when ether is added to the CH_2Cl_2 that remains after washing with water to reach a cloud point, a brown product precipitates. Filtration followed by the addition of more ether to the filtrate afforded the desired product in 30% yield.

Electrochemistry. Cyclic voltammetry, coulometry, and controlled-potential electrolysis were performed with a BAS-100 electrochemical analyzer. The working electrode for cyclic voltammetry was a platinum-inlay electrode (Beckman), and the auxiliary electrode was a platinum grid. The working electrode for bulk electrolysis was a 25-cm² platinum grid, and the auxiliary electrode was a carbon rod. The reference electrode in all electrochemistry experiments was a saturated calomel electrode (SCE). All solutions were degassed with argon.

Physical Measurements. Infrared (IR) spectra were recorded as Nujol mulls on a Perkin-Elmer 180 infrared spectrophotometer. Proton-decoupled ³¹P and ¹³C NMR spectra were recorded on a JEOL FX90Q Fourier transform spectrometer. The ¹³C NMR spectra were measured at 22.51 MHz with $(\text{CH}_3)_4\text{Si}$ as an external reference, and the ³¹P NMR spectra were obtained at 36.19 MHz with 85% H_3PO_4 as the external reference. All spectra were obtained at ambient temperatures.

Single-Crystal X-ray Analysis.⁸ The ruby-colored prismatic crystals of $\text{Rh}_2(\mu\text{-Ph}_2\text{Ppy})_2(\mu\text{-NO}_3)(\text{CO})\text{Cl}_2 \cdot \text{CH}_2\text{Cl}_2$ were grown by the slow diffusion of ether into a CH_2Cl_2 solution of **2**. A representative crystal was surveyed, and a 1-Å data set (maximum $(\sin \theta)/\lambda = 0.5 \text{ \AA}^{-1}$) was collected. Crystal parameters are listed in Table I. Atomic scattering factors were taken from ref 9 except those for hydrogen, which were taken from Stewart, Davidson, and Simpson¹⁰ and those for rhodium, which were taken from Cromer and Mann.¹¹ All crystallographic calculations were facilitated by the CRYM system.¹² All diffractometer

- (a) University of Tennessee. (b) North Carolina State University. (c) Formerly of North Carolina State University; currently at Pfizer Pharmaceutical.
- The groups of the periodic table are numbered according to recent recommendations from the IUPAC and ACS committees on nomenclature.
- Farr, J. P.; Olmstead, M. M.; Hunt, C. H.; Balch, A. L. *Inorg. Chem.* **1981**, *20*, 1182.

- Balch, A. L.; Guimerans, R. R.; Linehan, J.; Wood, F. E. *Inorg. Chem.* **1985**, *24*, 2021.
- Olmstead, M. M.; Balch, A. L. *J. Am. Chem. Soc.* **1976**, *98*, 2354.
- Balch, A. L.; Labadie, J. W.; Delker, G. *Inorg. Chem.* **1979**, *18*, 1224.
- Mann, F. G.; Watson, J. *J. Org. Chem.* **1948**, *13*, 502.
- Space group $P2_1/c$; $a = 11.863$ (8), $b = 17.076$ (5), $c = 19.430$ (8) Å; $Z = 4$; Syntex P1 diffractometer; $\text{Mo K}\alpha$, $\lambda = 0.71069$ Å; 3577 reflections, $I > 1.0\sigma(I)$; 469 parameters; $R = 0.046$. Other crystal data and refinement details are available as supplementary data.
- International Tables for X-ray Crystallography*; Kynoch: Birmingham, England, 1962; Vol. III, pp 204, 214.
- Stewart, R. F.; Davidson, E. R.; Simpson, W. T. *J. Chem. Phys.* **1965**, *42*, 3175.
- Cromer, D.; Mann, J. B. Report LA-3816; Los Alamos Scientific Laboratory: Los Alamos, NM, 1976.